Journal of the Korean Physical Society, Vol. 45, December 2004, pp. S728∼S731

Selective Formation of Si Nanocrystals by Assist Ion Beam Irradiation

Jae Kwon Kim, Kyu Man Cha, Jung Hyun Kang, Young Dae Kim,
Yong Kim,* Hong Jun Bark, Jae-Yel Yi and Tae Hun Chung
Department of Physics, Dong-A University, Busan 604-714

The deposition of substoichiometric SiO_x films is investigated by means of dual ion beam deposition with emphasis on assist ion beam irradiation effect. Linear dependence of oxygen content, x, on oxygen partial pressure is found. Preferential sputtering of Si phase over SiO_2 phase during assist ion beam irradiation has the effect of increasing the oxygen content in the ion-beam exposed region. The property indicates the lateral modulation of oxygen content of SiO_x film by inserting a shadow mask in the assist ion beam during deposition. The area-selective formation of Si nanocrytals is shown by photoluminescence measurements after post-deposition annealing.

PACS numbers: 78.55.-m, 78.67.Bf, 68.37.Lp, 81.07.Bc
Keywords: Ion beam sputtering, Nanocrystals, Photoluminescence, Selective formation

I. INTRODUCTION

Since the first discovery of light emission from porous silicon [1], the interest toward Si-based optoelectronics has rapidly increased. Due to better compatibility with standard ultra-large scale integrated circuit (ULSI) processes, Si nanocrystals in a dielectric matrix have gained much interest [2]. The various attempts at the deposition of SiO_x films include ion implantation [3], chemical vapor deposition (CVD) [4–6], reactive evaporation [7], co-sputtering [8], and ion beam sputtering [9], *etc.* Annealed SiO_x films yield highly luminescent nanocrystals with large density, regardless of deposition methods. The luminescence has been attributed to the quantum size effect of carriers confined in nanocrystals. The previous methods are not area-selective, and thereby nanocrystals are precipitated in the whole deposited area. However, the area-selective technique for Si nanocrystal formation may offer a processing flexibility in future ULSI processes with nanocrystal light emitting devices.

Weissmantel first used dual ion beam deposition (DIBD) [10] for reactive compound deposition. A DIBD system usually comprises two ion-beam sources. The primary source serves as a sputtering ion source and the other is utilized as an assist ion source. The assist ion beam has been utilized to significantly enhance and control the film properties. The effect of assist ion beam irradiation is the densification of film and the reduction of film stress. This is due to the fact that assist ions preferentially sputter deposits and contaminants with lower bonding energies than that of host material. Recently Lambrinos *et al.* [11] investigated the electrical properties of SiO_2, SiO_xN_y and SiN_x films deposited by DIBD. Reactive assist ions of N_2 have been used instead of inert ions. Ray *et al.* have observed the modification of refractive indices of films by varying assist ion energy during SiO_xN_y deposition [12]. The possibility of the area-selective control of film properties has been shown by Weissmantel [10]. By shadowing a region of substrate from a nitrogen ion beam, area-selective modification of film properties has been achieved. In this paper, we employ a similar idea, but extend it to the area-selective formation technique of Si nanocrystals by using ion beam irradiation during DIBD.

II. EXPERIMENTAL DETAILS

SiO_x films were deposited by employing a DIBD system. The DIBD system consists of two Kaufman-type broad-beam ion sources. Ultra-pure Ar gas was used for source gas for ion-beam generation. A primary ion source of 2.5 cm diameter with an incidence angle of 65° served as a sputtering ion source. P-type (100) silicon wafer (resistivity ∼10 Ωcm) was used as a sputtering target. The beam energy and beam current of the primary ion source were 750 eV and 7 mA, respectively. An assist ion source of 6 cm diameter with an incidence angle of 37° was used. The beam current of the assist ion source was 10 mA, and the beam energy was a variable parameter (0 ∼ 200 eV). 10 % Ar-diluted O_2 gas was introduced into the deposition chamber for a reactive deposition. The operating pressure was kept at 6 × 10^{-4} Torr while the partial pressure of O_2 gas was

*E-mail: yongkim@daunet.donga.ac.kr

varied. No intentional heating was applied to the substrate during deposition. SiO_x films were deposited for $2 \sim 4$ hours on 3-inch p-type (100) Si wafer (resistivity ~ 10 Ωcm) after a standard cleaning sequence to remove organic and inorganic surface contaminants. Deposited SiO_x films were subsequently annealed at 1100 °C for 2 hours in N_2 ambient. They were further annealed at 450 °C for 3 hours in a forming gas (N_2 90 %, H_2 10 %) for H_2 passivation. Photoluminescence (PL) was excited by a 488-nm Ar^+ ion laser (30 mW and $\sim$ 1 mm beam diameter) mechanically chopped at a frequency of 500 Hz. PLs were dispersed by a 0.5 m monochromator (Dongwoo optron DM500). The PL signal was detected by a photomultiplier tube (Hamamatsu R928) by using a standard lock-in technique (Stanford Research SR810). The observed PL spectra were corrected by using a tungsten-halogen lamp. All measurements were made at room temperature. The cross-sectional transmission electron microscope (TEM) image was observed by using JEOL JEM-2010 equipment through a standard preparation technique. The bonding configurations in oxide matrix were measured by Fourier-Transform infrared spectroscopy (FTIR, Biorad Excalibur FTS-3000). According to Pai *et al.* [13], Si−O−Si stretching vibration frequency shifts linearly with the oxygen content, x, provided that the film is homogeneous. Therefore, the oxygen content, x, in SiO_x film is determined from the position of the Si−O−Si stretching vibration frequency.

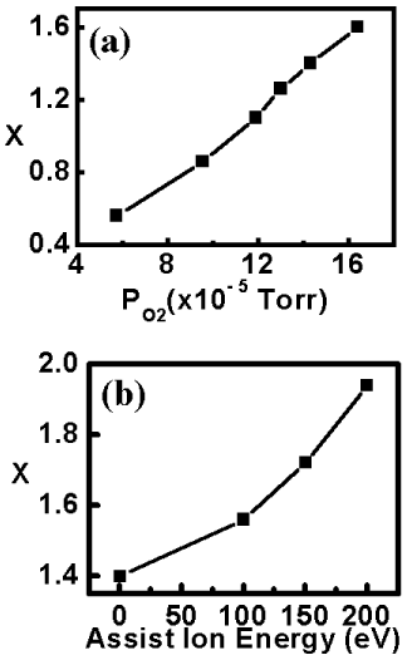

Fig. 1. (a) Variation of x as a function of oxygen patial pressure and (b) variation of x as a function of assist ion beam energy

III. RESULTS AND DISCUSSION

First, we grow several SiO_x films ($0.56 \leq x \leq 1.6$) with varying oxygen content by adjusting O_2 partial pressure ($P(O_2)$) from 0.6×10^{-5} Torr to 1.6×10^{-5} Torr. In this case, the assist ion source is not activated. The IR band found at around 1050 $\sim$1080 cm^{-1} is attributed to Si−O−Si stretching vibration. Si−O−Si stretching vibration frequency systematically shifts toward higher frequency on increasing $P(O_2)$. In addition, narrowing of the width of Si−O−Si stretching vibration is found indicating reduced randomness of Si−O bonding configurations. Then we activate the assist ion beam. Si−O−Si stretching vibration frequency shifts toward higher frequency on increasing the energy of assist ions. Figure 1 shows figure summarizing the variations of oxygen content, x, as functions of $P(O_2)$ and assist ion energy, respectively. From Figure 1(a), the oxygen content is linearly proportional to $P(O_2)$. Therefore, DIBD technique is quite reliable in preparing SiO_x films with desired oxygen content. Figure 1(b) shows the superlinear increase of x with ion beam energy and the film grown with $P(O_2) = 1.4 \times 10^{-5}$ under 200 eV ion beam irradiation is fairly close to stoichiometric SiO_2 film.

Microstructure of SiO_x films has been discussed either by the random mixture model (RMM) [14] or by the random bond model (RBM) [15]. As discussed by Lombardo *et al.* [16] from the detailed X-ray photoelectron spectroscopy study, only a combined model reflecting both models accounts for the true microstructure of SiO_x film. The tendency observed in Figure 1(b) is explained in terms of the preferential sputtering of Si phase due to higher sputtering yield as compared to SiO_2 phase when considering RMM as the microstructure of SiO_x film. The other possibility is due to the enhancement of the surface process which increase the rate of oxygen incorporation. However, we observe a significant reduction of film thickness with assist ion beam irradiation. The model of preferential sputtering would be more plausible. After post-deposition annealing, we observe PL emissions for samples in the compositional window of $1.1 \leq x \leq 1.4$ as shown in Figure 2. The size of Si crystallites critically depends on oxygen content in the film, and exceeds the size of nanocrystals through having appreciable quantum confinement effect for the films with $x < 1.1$. On the other hand, the small optical volume of nanocrystals for the films with $x > 1.4$ is not sufficient to yield reasonable PL intensity. As observed in Figure 2, PLs show a blue shift on increasing x. This is due to the stronger quantum confinement effect on decreasing the size of Si nanocrystals. Figure 3 shows a cross-sectional TEM image of several nanocrystals ($\sim$ 5-nm diameter) in $SiO_{1.26}$ film and supports the idea that observed PL is attributed to Si nanocrystals in the films. The samples with oxygen content x = 1.4 when non-irradiated, will not exhibit any ap-

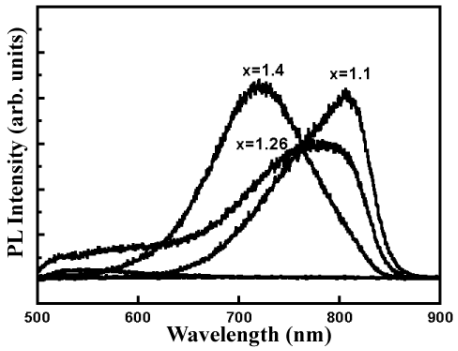

Fig. 2. PL spectra of SiO_x films with varying oxygen content, x, after high-temperature annealing.

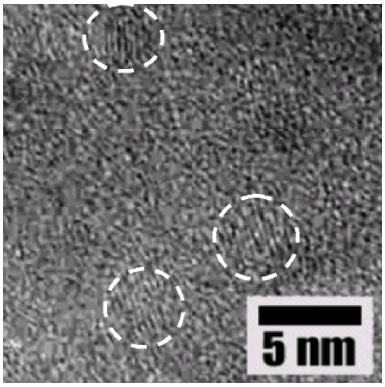

Fig. 3. Cross-sectional TEM image of $SiO_{1.26}$ film containing nanocrystals. White boundaries in the inset are guides to the eyes

preciable PL after ion beam irradiation, because $x > 1.4$.

The controllability of x in SiO_x films by assist ion beam irradiation can be utilized for area-selective formation of Si nanocrystals. A shadow mask is inserted in the assist ion beam. The mask is grounded to prevent a charging effect. Otherwise, assist ions would be repelled by Coulomb repulsion. A preliminary experiment employs a mask having 3 rectangular holes, and an ion beam with 200-eV ion energy is directed to a 3-inch Si wafer through the holes during DIBD. Figure 4 shows PL spectra recorded from the different parts of the 3-inch SiO_x sample after the deposition of SiO_x with the same partial pressure as the $SiO_{1.4}$ sample in Figure 2. The inset in Figure 4 shows a photograph of the 3-inch SiO_x sample. Due to the refractive-index alteration by ion-beam irradiation, the mask pattern is clearly discernible to the naked eye. However, the pattern is distorted, and specifically the pattern of the non-irradiated region is narrowed due to the significant spread of assist ions after escaping from the rectangular hole. The PL spectrum from the non-irradiated region shows maximum intensity at 615 nm and is blue-shifted by 115 nm as compared to PL from the $SiO_{1.4}$ sample shown in Figure 2. The result indicates that the nominally non-irradiated region

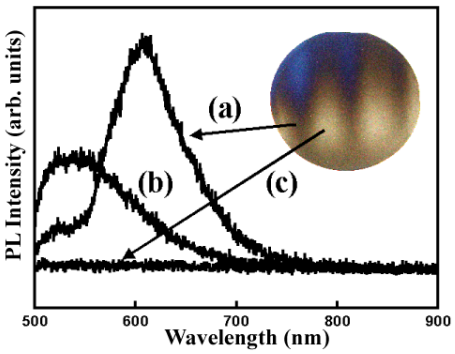

Fig. 4. PL spectra recorded from the different parts of 3-inch sample grown with a shadow mask. O_2 partial pressure is 1.4×10^{-5} Torr. The inset is the photograph of 3-inch sample. (a) and (c) are non-irradiated and irradiated regions, respectively. (b) is the transition region between (a) and (c)

is actually affected by ion-beam irradiation resulting in an increase of x. The central part of the irradiated region shows no PL, as expected. The transition region between non-irradiated and irradiated regions shows PL centered at 550 nm. The utilization of oxygen ions instead of inert Ar ions for assist ions may result in better area selectivity. However, the high reactivity of oxygen has led to early failure of the tungsten filament of the assist ion source. The sustainable time of the tungsten filament was usually less than an hour and did not allow repeatable investigations.

IV. CONCLUSION

We have investigated the deposition of SiO_x films ($0.56 \leq x \leq 1.94$) by the DIBD technique. We have shown the advantage of DIBD in preparing SiO_x films with desired oxygen content, x, by the adjusting oxygen partial pressure. We have observed the intense PL from SiO_x samples with oxygen content, x, in the narrow range of $1.1 \leq x \leq 1.4$, after post-deposition annealing at 1100 °C. The formation of Si nanocrystals responsible for PL has been confirmed by cross-sectional TEM observation. In addition, we have investigated the assist ion beam irradiation effect during deposition. Preferential sputtering of Si phase during assist ion beam irradiation increases the oxygen content, x, in the ion-beam exposed region. This property was utilized for achieving the area-selective formation of Si nanocrytals by inserting a shadow mask in the assist ion beam during deposition. Though preliminary results show a spread of the ion beam and distortion of the exposed pattern, the technique developed here may offer a process advantage during future ULSI processes when optimized.

ACKNOWLEDGMENTS

This work was supported by Grant No. R05-2002-000065-0 from the Basic Research Program of the Korea Science and Engineering Foundation.

REFERENCES

[1] L. T. Canham, Appl. Phys. Lett. **57**, 1046 (1990).
[2] J. K. Kim, H. J. Cheong, K. H. Park, Y. Kim, J-Y. Yi, H. J. Bark, S. H. Bang and J. H. Cho, J. Korean Phys. Soc. **42**, 316 (2003).
[3] S. K. Min, K. V. Shcheglov, C. M. Yang, H. Atwater, M. L. Brongersman, and A. Polman, Appl. Phys. Lett. **69**, 2033 (1996).
[4] J. H. Shin, H. S. Han, S. Y. Seo, and W. H. Lee, J. Korean Phys. Soc. **34**, 16 (1999).
[5] S. Lombardo, S. Coffa, C. Bongiorno, C. Spinella, E. Castagna, A. Sciuto, C. Gerardi, F. Ferrari, B. Fazio and S. Privitera, Mat. Sci. Eng. B **69-70**, 295 (2000).
[6] H. J. Cheong, J. H. Kang, J. K. Kim, Y. Kim, J-Y. Yi, T. H. Chung and H. J. Bark, Appl. Phys. Lett. **83**, 2922 (2003).
[7] M. Zacharias, J. Heitmann, R. Scholz, U. Kahler, M. Schmidt and J. Blasing, Appl. Phys. Lett. **80**, 661 (2002).
[8] M. Fujii, S. Hayashi and K. Yamamoto, Jpn. J. Appl. Phys. **30**, 687 (1991).
[9] J-S. Bae, S-H. Choi, K. J. Kim and D. W. Moon, J. Korean Phys. Soc. **43**, 557 (2003).
[10] C. Weissmantel, Thin Solid Films **32**, 11 (1976).
[11] M. F. Lambrinos, R. Valizadeh and J. S. Colligon, Nucl. Instr. and Meth. in Phys. Res. B **127/128**, 369 (1997).
[12] S. K. Ray, S. Das, C. K. Maiti, S. K. Lahiri and N. B. Charkrabarti, Appl. Phys. Lett. **58**, 2476 (1991).
[13] P. G. Pai, S. S. Chao, Y. Takagi and G. Lucovsky, J. Vac. Sci. Technol. A **4**, 689 (1986).
[14] H. R. Philipp, J. Non-Cryst. Solids **8-10**, 627 (1972).
[15] R. J. Temkin, J. Non-Cryst. Solids **17**, 215 (1975).
[16] S. Lombardo and S. U. Campisano, Mat. Sci. Eng. R **17**, 281 (1996).